

## The precision movement of upconversion nanoparticles on a surface by using scanning probe microscopy

© A.P. Chuklanov, A.S. Morozova, N.I. Nurgazizov, E.O. Mityushkin, D.K. Zharkov, A.V. Leontyev, V.G. Nikiforov

Zavoisky Physical-Technical Institute, FRC Kazan Scientific Center of RAS,  
420029 Kazan, Russia  
e-mail: achuklanov@kfti.knc.ru

Received April 18, 2023

Revised April 18, 2023

Accepted April 18, 2023

The possibility of precise movement of  $\text{YVO}_4:\text{Yb,Er}$  nanoparticles was studied in this work. Such nanoparticles exhibit upconversion luminescent properties and can serve as an accurate low-invasive probe of changes in the local parameters of the medium (in particular, temperature). Using an atomic force microscope, the substrate region with upconversion nanoparticles deposited from the solution and accompanying residues of the synthesis products was cleaned. The use of mechanical marks on the substrate made it possible to compare the atomic force and optical confocal images of the surface and to register the luminescence from an individual nanoparticle. Elemental analysis and luminescence spectra unambiguously identify the nanoparticle as  $\text{YVO}_4:\text{Yb,Er}$ .

**Keywords:** upconversion nanoparticles, scanning probe microscopy, luminescence.

DOI: 10.61011/TP.2023.07.56644.82-23

### Introduction

Luminescent nanoparticles with an upconversion type of excitation, when two low-energy photons in the infrared (IR) range are absorbed and a photon of the visible spectrum is emitted, are used to solve many problems. In particular, due to the unambiguous dependence between the intensity of luminescent lines on temperature, such nanoparticles can be used as hypersensitive thermometers with high spatial and temporal resolution. The use of near-IR radiation for excitation has a number of advantages that may prove decisive in some scientific fields. These include: high optical transparency in the near IR range of silicon and biological tissues, absence of parasitic luminescence, significant reduction of local heating by pumping radiation [1]. When such upconversion nanoparticles (UNP) are used as thermosensors, the temperature is measured by registering the ratio of line intensities in the spectrum of rare earth ions, which is the simplest and most accurate method for remote measurement.

Spintronics, one of the actively developing areas of solid state physics, can become a very promising area of application of the UNP as a local temperature sensor. With this approach, the logic elements of micronanoelectronics are built using the electron spin transfer, and not its charge (as in conventional micronanoelectronics). One of the most important advantages of such devices is low power consumption and, as a result, low heat loss due to the small release of Joule heat. At the same time, it is necessary to use ferromagnetic materials as a source of spin-polarized electrons in spintronic devices. It is well known that the properties of low-dimensional ferromagnets differ markedly from the properties of bulk materials. In

particular, the Curie temperature at which the transition from the ferromagnetic to paramagnetic state takes place is markedly decreased for thin films. Therefore, it is necessary to control the temperature of spintronic devices both in space (different parts of ferromagnetic structures can heat up differently during operation due to boundary conditions) and in time during pulsed operation.

The upconversion system consists of two closely spaced rare earth ions. One of them is the ion of ytterbium  $\text{Yb}^{3+}$  that acts as a sensitizer. Its absorption cross-section at a wavelength of 980 nm is an order of magnitude higher than that of other rare earth ions. The second ion (it can be, for example,  $\text{Er}^{3+}$ ,  $\text{Tm}^{3+}$ ,  $\text{Ho}^{3+}$ ) is a radiating center with characteristic narrow lines in its emission spectrum. The excitation of the second ion occurs as a result of a twofold energy transfer from the excited ion of ytterbium  $\text{Yb}^{3+}$ , which determines the upconversion properties of the system from a pair of rare earth ions. The efficiency of the two-quantum excitation process is due to metastable excited levels (with submillisecond lifetimes) involved in energy transfer. In this regard, the correct choice of a matrix with low-energy phonons is of particular relevance to minimize undesirable non-radiative relaxation by a multi-phonon mechanism. As a rule, such matrices are oxide (for example, crystals  $\text{VO}_4$  with a phonon energy  $600\text{ cm}^{-1}$ ), or fluoride compounds (for example, crystals  $\text{NaF}_4$  with a phonon energy  $350\text{ cm}^{-1}$ ).

Note that modern measurement protocols determine temperature sensitivity based on the averaged characteristics of a large number of nanoparticles. It is important to emphasize here that the spectral properties of individual nanoparticles may differ greatly from the ensemble aver-

ages. The variation in the size and shape of the UNP associated with „wet“ synthesis technology determines a wide dispersion of photophysical properties. When using a large ensemble of UNP, for example, in the form of a film on the surface of a solid or in the form of a solution in a biological object, temperature measurement is not very difficult. However, local temperature measurement involves the use of a single UNP, the properties of which are likely to differ greatly from the ensemble averages. This feature is a serious obstacle to calibration, which hinders the development of mass technology for using anchors as thermosensors.

Many leading research groups in the world are engaged in the development of temperature nanosensors. The upconversion system  $\text{Yb}^{3+}$ ,  $\text{Er}^{3+}$  is considered one of the most promising for creating nanothermometers operating on the principle of fluorescent ratiometry, the main question is to choose a suitable matrix. For example, in the work [2], the authors develop thermosensors based on nanoparticles  $\text{SrF}_2:\text{Yb,Er}$ . The paper [3] proposes sensors based on nanoparticles  $\beta\text{-NaYF}_4:\text{Yb,Er}$  with the possibility of coating them with shells to improve upconversion efficiency, in the paper [4] a group of researchers is considering the possibility of using nanoparticles  $\text{YF}_3:\text{Yb,Er}$  as temperature nanosensors. According to our estimates, the most suitable approach based on oxide nanoparticles  $\text{YVO}_4:\text{Yb,Er}$  was proposed by scientists from the University of Texas [5], since such sensors are much less toxic compared to their fluoride counterparts.

The use of scanning probe microscopy (SPM) methods is one of the possible ways for manipulating nanoparticles. The family of SPM methods has proven to be a fast, accurate and inexpensive way to study surface topography in various media (from liquid to ultra-high vacuum) and at various temperatures (from fractions to about a thousand degrees Kelvin). In addition to the „usual“ usage described above, the SPM has many modifications. In particular, magnetic force microscopy makes it possible to obtain the distribution of magnetic moments in the near-surface layer of ferromagnets with a resolution unattainable in Kerr optical microscopy. Probe lithography makes it possible to produce planar structures of complex shape on the surface by mechanically moving the probe and/or passing an electric current. SPM is ideal for manipulating objects on the surface in the size range from units of microns to tens of nanometers. At the same time, it is possible both to move surface objects with *ex-situ* condition monitoring by the probe, and to apply particles to the surface from the surface of a specially prepared probe. SPM can be used to apply nanoparticles to the surface of spintronic devices with the desired density. Or it can be used for selection of nanoparticles by spectral characteristics (using confocal spectroscopy). SPM allows controlling the geometric parameters of nanoobjects and their location on the surface with nanometer accuracy, which should allow (together with confocal spectroscopy) selecting UNP based on the spectral characteristics.

In this paper, the problem of selection of UNP based on size was solved by using the combined methods of atomic force microscopy (AFM) and optical confocal microscopy (OCM). AFM was used for visualization and control of UNP movement on the surface, OCM was used for visualization and investigation of luminescent properties.

## 1. Specimen preparation and study methods

The synthesis of UNP  $\text{YVO}_4$  doped with  $\text{Er}^{3+}$  and  $\text{Yb}^{3+}$  was performed using the hydrothermal method, which is described in [6–8]. Aqueous solutions of  $\text{Y}(\text{NO}_3)_3$ ,  $\text{Er}(\text{NO}_3)_3$  and  $\text{Yb}(\text{NO}_3)_3$  with concentrations of 0.1, 0.002 and 0.02 mol/l, respectively, were slowly added to the aqueous solution of  $\text{Na}_3\text{VO}_4$  with a concentration of 0.1 mol/l with constant stirring at room temperature. As a result, an UNP colloidal solution in water was produced, a drop of which (volume  $5\ \mu\text{l}$ ) was applied to the substrate and dried [9]. An optically polished slide with a thickness of  $300\ \mu\text{m}$  with pre-mechanically applied micro-scratch marks was used as a substrate. They were applied parallel to the faces of the substrate and formed an irregular rectangular grid. The width, depth and distance between the micro-scratches were selected in such a way that they could be visualized simultaneously in AFM and OCM. Thus, AFM and UNP optical images can be compared. This approach has proven itself well in the study of the morphology of various structures on a wide range of substrates [10,11]. The substrates had a noticeably elongated rectangular shape for ease of fixation in AFM and OCM, the typical lateral size is  $5 \times 12\ \text{mm}$ . A drop of colloidal solution containing UNP was applied in such a way that at least one intersection of micro-scratches was in the application area. The area of the substrate covered with UNP was approximately 50% of the area of the entire substrate, the edges of the dried drop of colloidal solution were always clearly visible in an optical microscope, which significantly facilitated the primary positioning in AFM. Solver-Bio AFM (NT–MDT), combined with a conventional optical microscope, was used to manipulate the UNP, which allowed choosing a location for AFM manipulations near micro-scratches. Maximum lateral AFM scanning field:  $100 \times 100\ \mu\text{m}$ . Maximum scanning depth along  $z$ :  $5\ \mu\text{m}$ . Since the UNP luminescence can also be excited by ultraviolet laser pumping, when photons are absorbed directly by the matrix, and then the energy is transferred to the ion  $\text{Er}^{3+}$  without the participation of ytterbium ions  $\text{Yb}^{3+}$ , to simplify the positioning process, it was decided to supplement the illumination system of a conventional optical microscope with a SONY SLD3232VF laser diode, emitting at a wavelength of 405 nm, together with an interference light filter felh0500 (Thorlabs, inc.) to cut off pumping in front of the detector. N11-A AIBA probes with a hardness of 3 N/m and a resonant frequency of 60 kHz were used. This type of probes can be attributed to „soft semi-contact probes“, when the probe makes forced

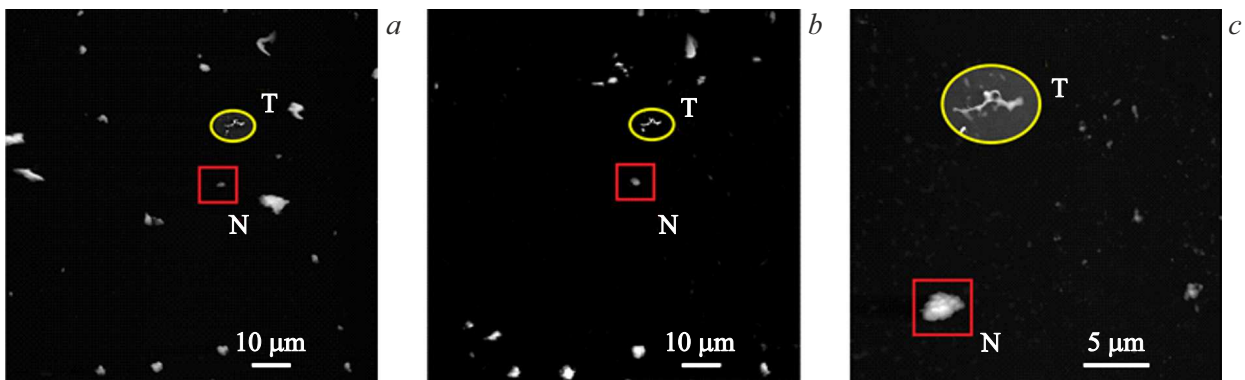


**Figure 1.** AFM images acquired in semi-contact mode of the surface area with UNP: *a* — initial, height range  $2.8\ \mu\text{m}$ ; *b* — after clearing the AFM probe in contact mode, height range  $1.8\ \mu\text{m}$ ; *c* — after clearing and increasing, the height range is  $0.7\ \mu\text{m}$ . The rectangular area „N“ contains a candidate microparticle from which the luminescence spectrum is registered. An oval area of the surface „T“ with a characteristic shape defect, which remained unchanged during the manipulation of objects on the surface, was used as a marker during positioning. The local contrast of the region *T* is increased for clarity.

oscillations at its own frequency in semi-contact mode, slightly touching the surface. At the same time, the AFM feedback registers a change in the amplitude of the probe oscillations. This mode of operation is characterized by a small force of interaction with the surface and is well suited for obtaining high-quality images of topography with high lateral resolution, while all objects on the surface remain in their places without moving. A force of interaction with the surface of  $> 10^{-6}\ \text{N}$  can be achieved in contact mode owing to the rigid and short beam of the cantilever[12]. Thus, it is possible to visualize the surface and manipulate objects on it with one probe. With this approach, the accuracy and overall speed of measurements and manipulations are significantly increased, since there is no need to change the probe, adjust, move to the sample surface, etc. The area of the surface within which AFM manipulations were performed was additionally monitored visually using a conventional optical microscope.

The luminescent properties of the UNP were studied using self-assembled OCM. The ANF luminescence was excited by a MicronLux laser with a wavelength of 980 nm and a power of 100 mW. The pump beam was focused with a 100x lens, the diameter of the constriction was  $1\ \mu\text{m}$ . The luminescent radiation was collected with a lens  $\text{NA} = 0.70$  from the upper surface of the sample, where the anchors were located. A dichroic mirror and a FELH-800 filter were used to separate the luminescence from the pump radiation. The filtered radiation was input into a multimode fiber using an aspherical short-focus lens and it was output using a 4x micro lens, after which it was focused by a long-focus lens on the entrance slit of the M266 monochromator. The recording of luminescence spectra had the following characteristics: exposure — 34 s, number of frames used in averaging, — 74, width of the entrance slit —  $400\ \mu\text{m}$ . The luminescence spectra were adjusted taking into account the signal recorded on a transparent quartz plate.

## 2. Results and discussion

The finished sample was placed in the AFM and the UNP manipulation algorithm consisted of several successive stages:

1) at first, a suitable location was selected using the Solver-Bio AFM optical microscope. At the same time, several conditions had to be met: the place for manipulating the UNP should be near (less than  $100\ \mu\text{m}$ , which is the maximum area of lateral AFM scanning) the area of intersection of the marks- micro scratches on the substrate; illumination from downconversion luminescence in this area should not be too strong (controlled visually), large objects should not be visually observed in the scanning area;

2) the AFM image of the surface was recorded in semi-contact mode with the largest possible lateral scanning field (Fig. 1, *a*). It is important to note that at this stage there was no unambiguous correspondence between the topography of surface objects and their luminescent properties;

3) Then a suitable candidate object was selected, for example, the object „N“ (Fig. 1, *a*). Among the criteria that the candidate object should satisfy, it is possible to distinguish a height of no more than 100–200 nm and a high-quality AFM image. The lateral dimensions of objects cannot be used as a reliable selection criterion considering that the probe is under strong pressure during surface cleaning (at stage 4) and the control of its shape in the process is very difficult, due to the convolution effect. The presence of artifacts on the AFM image in the area of the object (for example, breaks or strong noises) may indicate sharply changed adhesive properties, which in turn is one of the indications of contamination of the surface;

4) The AFM was switched to the contact mode of operation, and a sequential series of scans was performed. At the same time, the starting point, the scan size and the scanning direction were selected in such a way that when the AFM probe moves, all objects, except for one selected

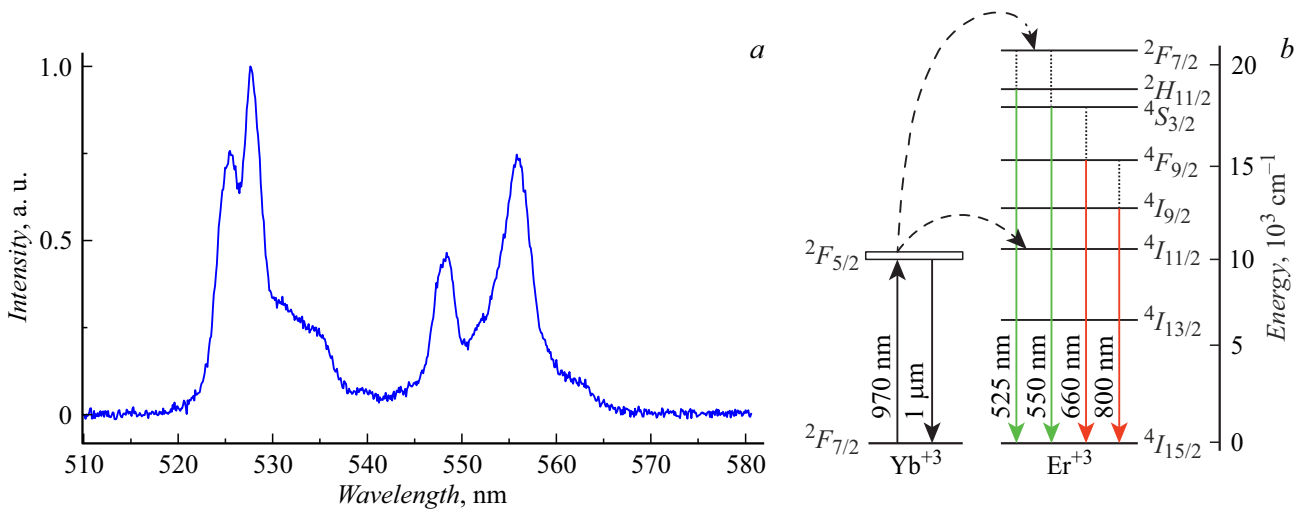


**Figure 2.** The luminescence spectrum of a single ANF under laser excitation at a wavelength of 980 nm (a) and a diagram of energy levels and energy transfer processes in upconversion particles. Solid arrows show radiative transitions, dotted arrows and lines show the energy transfer and non-radiative transitions (b).

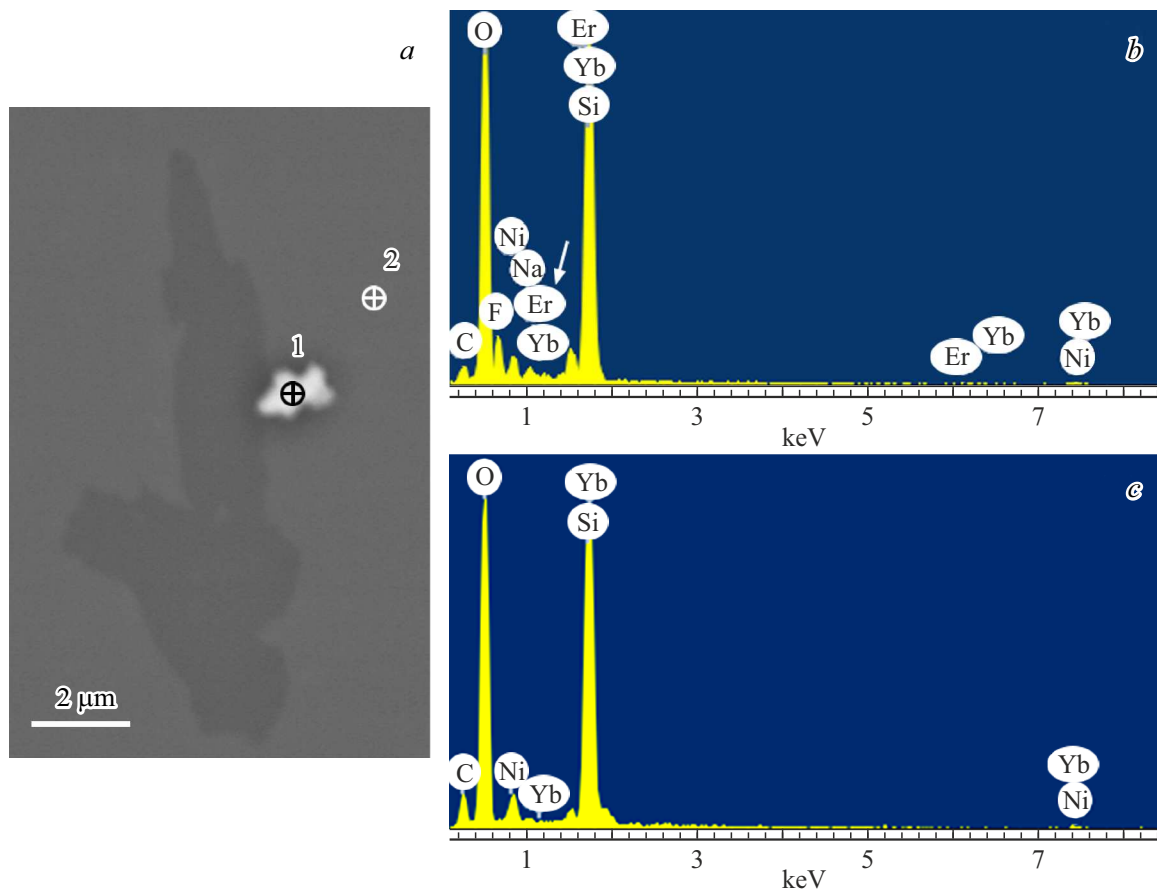


**Figure 3.** Scanning electron microscopy image (a) of a surface area after clearing, containing an UNP and 2 of the spectrum of elemental analysis. The spectrum (b) corresponds to the region 1, and the spectrum (c) corresponds to the region 2. A comparison of the spectra shows that Yb and Er ions are simultaneously present only in the 1 region, which is also a good indication that the object under study is an UNP. The pressure in the chamber  $4.8 \cdot 10^{-3}$  Pa, operating voltage 10 KV.

one, are pushed to the edge of the maximum permissible scanning field. The ultimate goal of the manipulations was to have only one desired object on the maximum available scan size;

5) The AFM returned to semi-contact operation mode to monitor the results obtained (Fig. 1, *b, c*). Steps 2–5 were repeated if necessary until a satisfactory result was achieved.

Then, the desired area was located in the OCM using micro-scratch marks and the luminescence spectrum from the candidate object was recorded. The constriction of the pump spot, much smaller than the area cleared on the AFM, reliably guaranteed that the luminescence spectrum was recorded exclusively from object N. The spectrum of upconversion luminescence when excited by a laser at a wavelength of 980 nm is shown in Fig. 2, *a*. The narrow lines correspond to the emission of erbium ions  $\text{Er}^{3+}$  from different excited states. Comparing the diagram of energy levels in Fig. 2, *b* and the luminescence spectra, it is seen that the bands in the 525, 550 nm regions correspond to the radiative transitions  ${}^2H_{11/2} - {}^4I_{15/2}$ ,  ${}^4S_{3/2} - {}^4I_{15/2}$  in erbium ions  $\text{Er}^{3+}$ . This also serves as a strong proof that the object N is a single nanoparticle  $\text{YVO}_4:\text{Yb,Er}$ .

Additionally, the sample was examined in a scanning electron microscope „EVO 50 XVP“ (Carl Zeiss) with a probe microanalysis system „INCA Energy–350“ (Oxford Instruments). The test sample was additionally coated with a nickel layer 5 nm thick to drain the charge. Previously applied micro-scratch marks were also used in the SEM to enter the place with a single UNP (Fig. 3, *a*). Elemental analysis has shown (Fig. 3, *b, c*) that the region inside the object N contains Yb and Er ions, while the substrate around does not.

## Conclusion

The paper presents and experimentally implements a method that allows manipulations with UNPs on the surface. It is based on a combination of AFM, OKM and SEM capabilities by synchronizing their scan areas. In particular, this allowed cleaning the surface from synthesized UNP, contaminants and associated residues of synthesis products and leave one selected UNP in the center. This manipulation made it possible to observe the luminescent signal directly from one UNP. This is a striking example of the spectroscopy of a single oxide UNP  $\text{YVO}_4:\text{Yb,Er}$ , which according to our data was performed for the first time. Thus, the proposed technique allows (i) studying the photophysical properties of nanoscale phosphors; and (ii) provides a tool for selecting nanoscale phosphors, manipulating and positioning them on the surface areas of interest.

## Acknowledgments

The authors thank N.M. Lyadov for taking measurements in a scanning electron microscope.

## Funding

This study was financially supported by the Russian Science Foundation (project №23-29-00516).

## Conflict of interest

The authors declare that they have no conflict of interest.

## References

- [1] C. Zaldo. *Lanthanide-based luminescent thermosensors: From bulk to nanoscale* (In book: Lanthanide-Based Multifunctional Materials) (Elsevier, Netherlands, 2018), p. 335–379. DOI: 10.1016/B978-0-12-813840-3.00010-7
- [2] S. Balabhadra, M.L. Debasu, C.D.S. Brites, R.A.S. Ferreira, L.D. Carlos. *J. Phys. Chem. C*, **121**, 13962 (2017). DOI: <https://doi.org/10.1021/acs.jpcc.7b04827>
- [3] K. Green, K. Huang, H. Pan, G. Han, Sh.F. Lim. *Front. Chem.*, **6**, 416 (2018). DOI: 10.3389/fchem.2018.00416
- [4] A. Ciric, J. Aleksic, T. Barudzija, Z. Antic, V. Dordevic, M. Medic, J. Perisa, I. Zekovic, M. Mitric, M.D. Dramicanin. *Nanomaterials*, **10** (4), 627 (2020). DOI: 10.3390/nano10040627
- [5] M.H. Alkahtani, C.L. Gomes, Ph.R. Hemmer. *Opt. Lett.*, **42** (13), 2451 (2017). DOI: 10.1364/OL.42.002451
- [6] G. Mialon, S. Turkan, A. Alexandrou, T. Gacoin, J.-P. Boilot. *J. Phys. Chem. C*, **113** (43) 18699 (2009). DOI: 10.1021/jp907176x
- [7] M.H. Alkahtani, F.S. Alghannam, C. Sanchez, C.L. Gomes, H. Liang, Ph.R. Hemmer. *Nanotechnology*, **27**, 485501 (2016). DOI: 10.1088/0957-4484/27/48/485501
- [8] A.G. Shmelev, V.G. Nikiforov, D.K. Zharkov, V.V. Andrianov, L.N. Muranova, A.V. Leontyev, Kh.L. Gainutdinov, V.S. Lobkov, M.H. Alkahtani, P.R. Hemmer. *Bull. Russ. Academy Sciences: Physics*, **84**, 1439 (2020). DOI: 10.3103/S1062873820120357
- [9] D.K. Zharkov, A.G. Shmelev, A.V. Leontyev, V.G. Nikiforov, V.S. Lobkov, M.H. Alkahtani, P.R. Hemmer, V.V. Samartsev. *Laser Phys. Lett.*, **17** (7), 075901 (2020). DOI: 10.1088/1612-202X/ab9115
- [10] M.A. Ziganshin, I.G. Efimova, V.V. Gorbachuk, S.A. Ziganshina, A.P. Chuklanov, A.A. Bukharaev, D.V. Soldatov. *J. Pept. Sci.*, **18** (4), 209 (2012). DOI: 10.1002/psc.1431
- [11] D.A. Bizyaev, A.A. Bukharaev, O.V. Ugryumov, O.A. Varnavskaya. *Proceedings of the 10th International Symposium „Nanophysics and Nanoelectronics“* (N. Novgorod, Russia, 2006), p. 177. (in Russian)
- [12] D.A. Bizyaev, A.A. Bukharaev, D.V. Lebedev, D.V. Nurgazizov, T.F. Khanipov. *Tech. Phys. Lett.*, **38** (7), 645 (2012). DOI: 10.1134/S1063785012070152

Translated by A.Akhtyamov